Measuring Slow Flows Using the Garfield Magnet

By Sebastian Richard
Supervisor: Dr. Ben Newling
Department of Physics, University of New Brunswick

– Summer 2017 –

Abstract
Nuclear Magnetic Resonance (NMR) has long been used for measuring flows as it has the unique advantage of being a truly non-invasive method for which to do so. In this report, we describe our efforts to apply this concept to a magnet with a large constant gradient in order to measure slow flows 0.0019—0.0244 m/s, with the goal of developing a flow measurement method that works well in a high gradient permanent magnet.

Garfield Magnet
The Garfield magnet[1,7] (figure 1) is a permanent magnet that consists of two identical, specially shaped magnetic lobes that are held in close proximity together by being bolted to a sturdy non-magnetic metal frame. In the region between the two lobes, the magnetic field has a large 12.9 T/m gradient in the upwards direction through the magnet. By using a magnet with a large gradient, it is possible to measure slow flow rates as the excited slice within the sample will be very thin and sensitive to the flow of magnetization out of the slice. The Garfield magnet is not ideal for measuring fast flows for the same reason. Most experiments were performed at or near 33.2 MHz which corresponds to the region between the two lobes where the field strength is ~0.78 T. The flow direction was in the same direction as the field gradient. The slice thickness S within the magnet can be determined from the RF pulse duration p, the gradient strength G, and the gyromagnetic ratio γ.

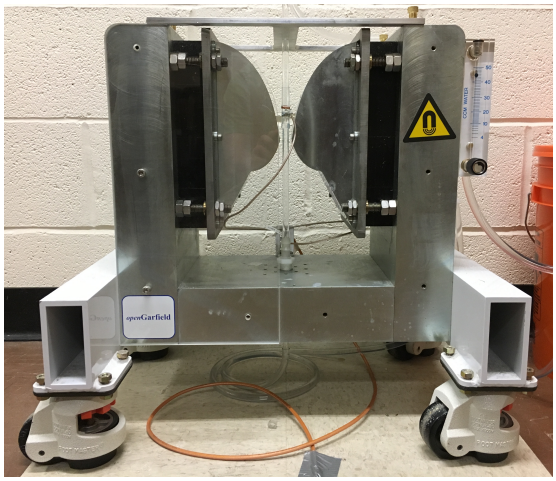

Figure 1: The Garfield magnet shown in it's configuration to measure flows.

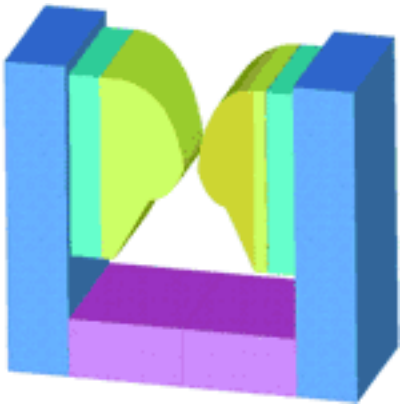

Figure 2: A simplified 3D rendering of the Garfield magnet (laplacian.co.uk)

$$S = \frac{p^{-1}}{G\gamma} \tag{1}$$

Flow Network
In order to make consistent flow measurements, a way of achieving a constant flow through the magnet was required. A gravity fed flow from a reservoir suspended several feet above the magnet that is replenished using a pump from another reservoir set at floor level was chosen. In order to maintain a

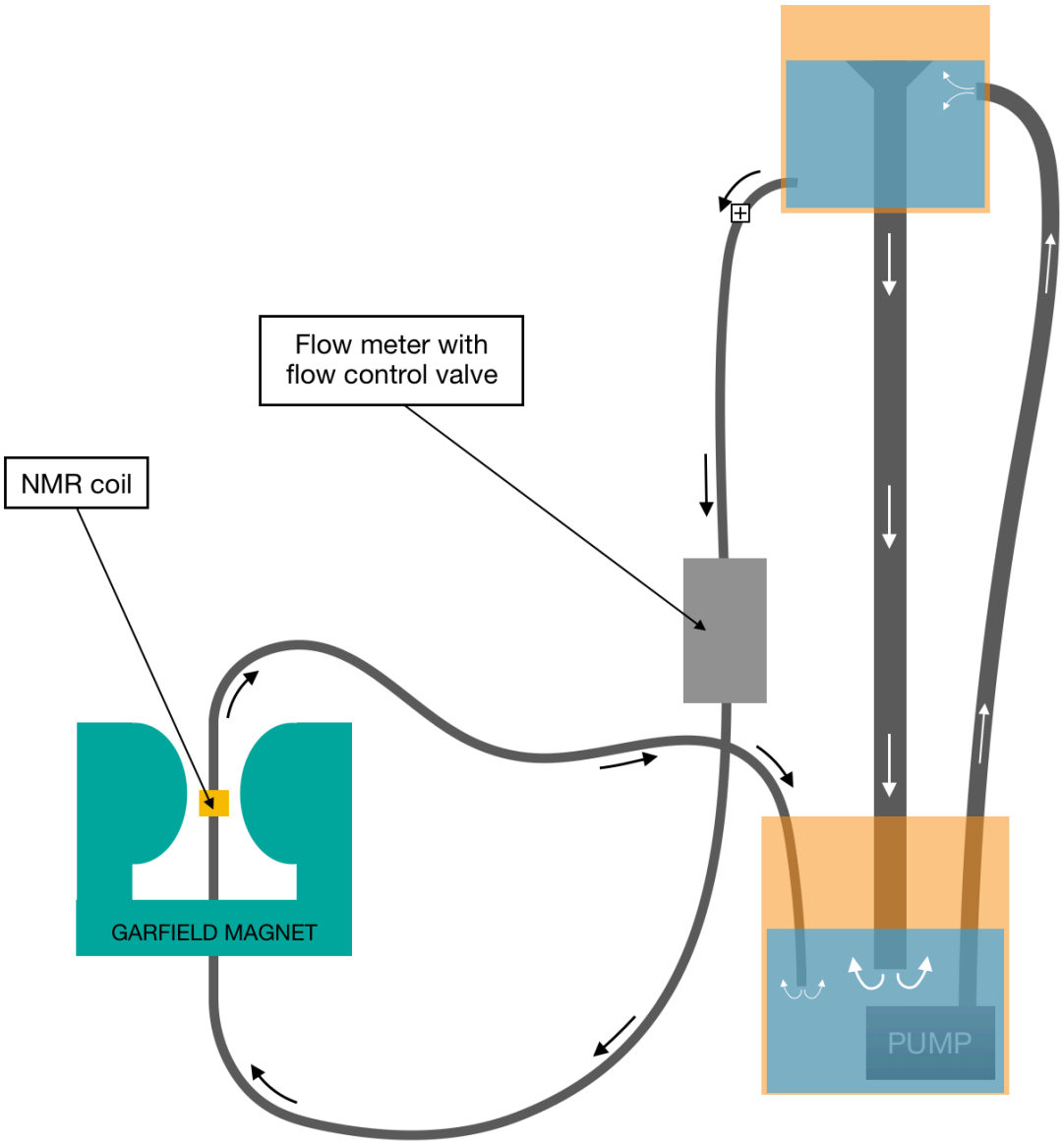

Figure 3: Diagram of the flow network. The two reservoirs are depicted in orange.

constant level in the upper reservoir (and therefore a constant head pressure though the magnet) the pump provided more inflow into the upper reservoir than was flowing through the magnet. An overflow was installed in the upper reservoir to return excess water to the lower reservoir. It was found that in order for the outflow to remain as constant as possible it should have a large diameter opening and run up vertically though the reservoir. A diagram of the flow network design is shown in figure 3. In order to precisely control the flow through the magnet, a flow meter purchased from Omega (model# FL-2045) was used to measure and set the flow rate. The meter was also used to calibrate the flow as measured using NMR techniques. Typical flexible tubing was used throughout the construction of the flow network except for the portion running though the magnet where a 70 cm length of glass tubing with an ID of 6.6 mm was used. A second shorter piece of glass tubing that could slide over the first length was acquired upon which to build the NMR coil. Various coil designs were tested and in the end a 1-turn copper tape solenoidal coil

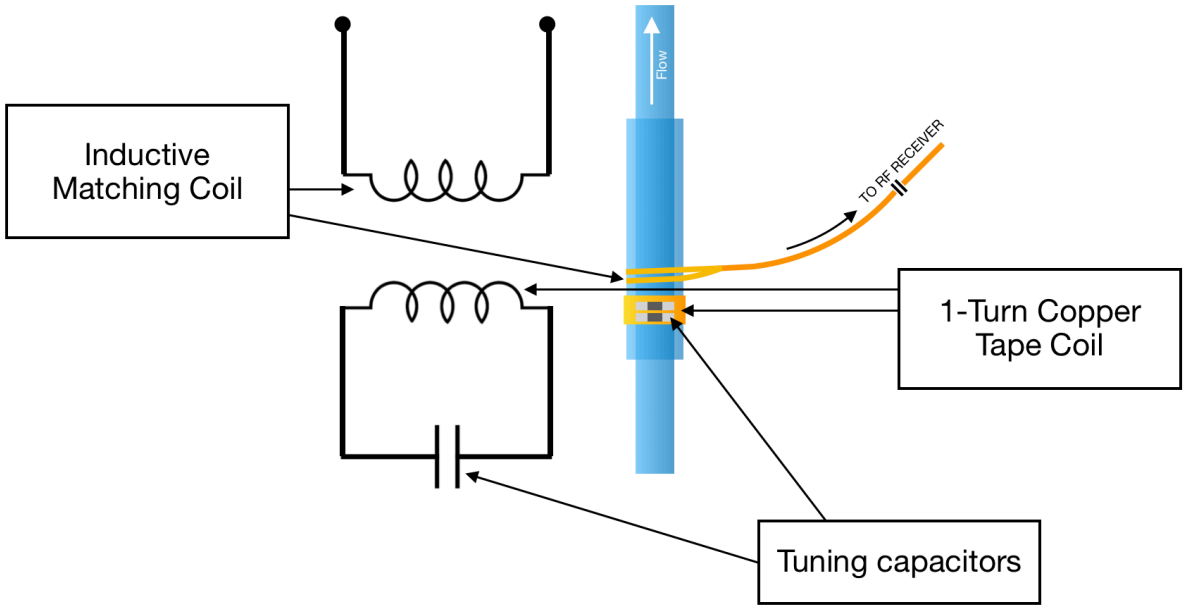

Figure 4: diagram of the NMR coil that was used. On the left is the coil represented in a circuit diagram and on the right the coil is shown as it is actually constructed.

was chosen[2] (figure 4) as the SNR proved to be best with this particular design. The coil is capacitively tuned and inductively matched, and is built directly onto the surface of the second (shorter) glass tube*.

Measurement

Data was acquired using the Carr-Purcell-Meiboom-Gill (CPMG) sequence (figure 5) which consists of a $90_x°$ pulse followed by a series of $180_y°$ pulses. Each $180_y°$ pulse refocuses the magnetization to obtain an

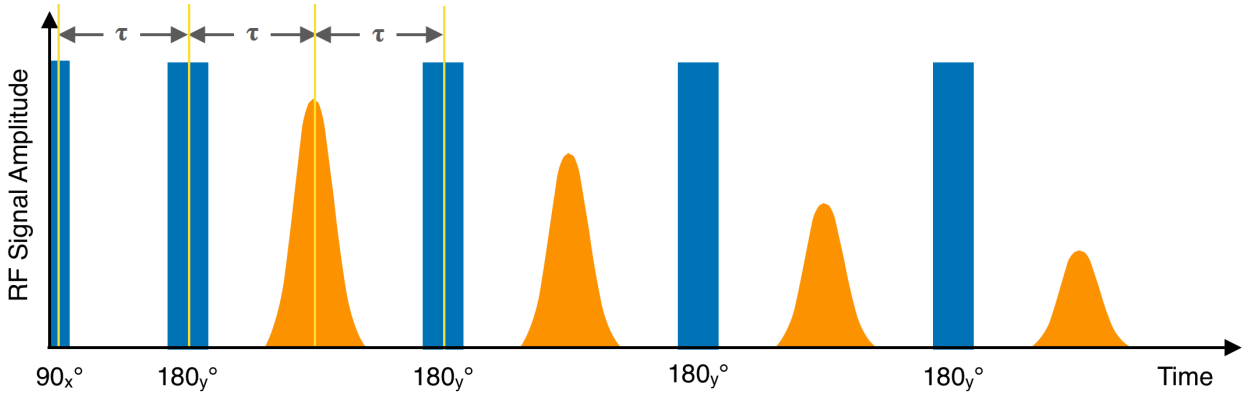

Figure 5: a diagram of a basic CPMG sequence. The RF pulses are represented in blue and the echoes in orange. τ denotes the time between the 90 and 180 RF pulses.

echo. The amplitude of the echoes decreases with each successive echo as a consequence of T_2 de-phasing[3] and as a result of movement of the magnetized portion of the sample out of the sensitive region (slice) of the detector due to flow. Data analysis was based off work done by Osán *et al.*[4] By comparing

* More details on the construction of the coil are provided in a separate document.

how echo amplitudes change with different flow rates it is possible to determine flow velocity. It can be shown that the signal intensity is proportional to the volume of excited sample in the slice.

$$Signal \propto V(0) = LS \tag{2}$$

And for plug flows:

$$V(t) = V(0) - Sv_{avg}t \tag{3}$$

Where $V(0)$ denotes the total fluid volume in the sensitive region of the coil when the CPMG sequence is started at time $t = 0$. V is the velocity of the fluid, L is the length of the $180_y°$ slice, and S is the cross sectional area of the flow. $V(t)$ can be expressed as

$$V(t) = V(0)\left(1 - \frac{v_{avg}}{L}t\right) \text{ which is in the form } Signal\ I = A + Bt. \tag{4}$$

Fitting the first few echoes of the echo train to the linear fit $I = A + Bt$ one can calculate the average flow velocity from

$$v_{avg} = \left(-\frac{B}{A}\right)L \tag{5}$$

However the value of L is very difficult to determine. One way to deal with this is to plot $-B/A$ values as a function of flow velocity (measured using an alternate method). L will be given by the slope of the resulting plot and its value can then be substituted into eq. 5. The value of L should be constant.

While the above is for plug flows, an assumption that was verified by Osán *et al.*[4] is that it also holds reasonably true for laminar flows which occur at slow flow velocities. The transition between laminar flow and plug flow can be determined by the Reynolds number (*Re*) which can be understood as the ratio between the inertial force and the viscous force and characterizes the friction effects of the fluid[4]. The Reynolds number is expressed as

$$Re = \frac{\rho v_{avg} d}{\eta} \tag{6}$$

where ρ is the fluid density, η is the dynamic viscosity, and d is the is the pipe diameter[4]. In these experiments the Reynolds number was calculated to be 13 at 4CCM and 160 at 50 CCM. The critical value of the Reynolds number (when the fluid will transition from laminar to turbulent flow) is around ~2300 for Newtonian fluids in flow through a cylindrical pipe[4].

As the flow velocity increased, it was observed that the difference between the amplitudes of the even and odd echoes increased (figure 5). As the flow increased, the amplitudes of the odd echoes decreased faster than the even echoes. This echo modulation is a result of even echo re-phasing[5,6] which occurs in the presence of a constant gradient. From visual inspection of the data, it was established that fitting the first five even echoes to a linear fit yielded the best results (figure 6).

In addition to signal attenuation due to flow, there is also be some attenuation as a result of T_2 effective. To remove this effect, the data was divided by a data set acquired for zero flow. By diving the flow data by the zero flow data, the effects of T_2 effective would be negated and the remaining reduction in signal intensity would be as a result of only the flow.

Results and Discussion

Data was acquired for 0.0019—0.0244 m/s flow rates several times for 4 different values of τ (40, 60, 150 and 240μs). For τ = 150 μs it was observed that the linear model given in equation 5 did not describe the data. Between 0.0097—0.014 m/s the -B/A *vs.* velocity plot would abruptly change direction (figure 8) both sections before and after the abrupt direction reversal however appear reasonably linear in some of the repeats. More research will need to be done to properly explain this. Interestingly, for all the other values of τ (40 and 60 and 240μs) this direction reversal was not observed. Visual inspection of the data in Matlab showed that a linear fit of the echoes proved inadequate in many cases (with R^2

Figure 6: 0.0244 m/s CPMG echo train for τ =150μs which shows the echo modulation starting with the 3rd echo. The first 5 even echoes are indicated by the red dots

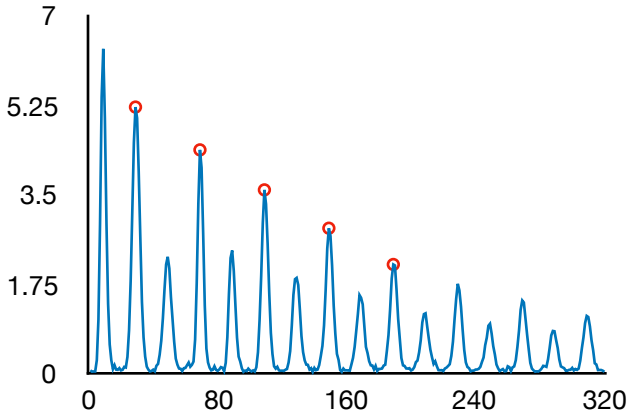

Figure 7: Plot of velocity vs. -B/A ratio for τ = 240 μs.

Figure 8: Plot of velocity vs. -B/A ratio for τ = 150 μs. Note the abrupt direction reversal. Repeats have shown this trend to be consistent.

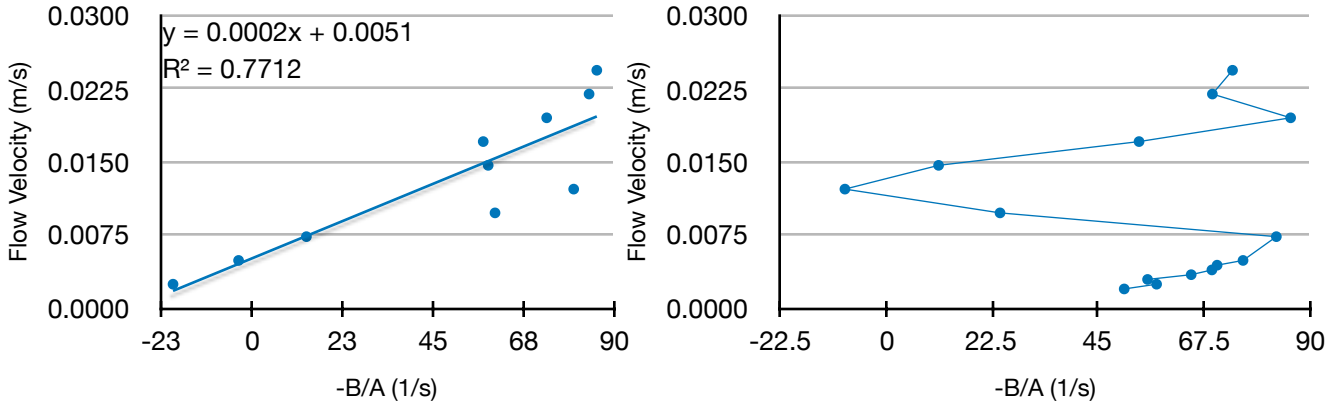

Figure 9: Plot of the velocity vs. the average -B/A of the first 3 repeats for τ = 40 μs with errors (left) and for τ = 60 μs (right). The error in the flow velocity is taken from the flow meter manufacture's specification and the errors in the -B/A ratios are calculated as the average standard deviation for the 3 repeats.

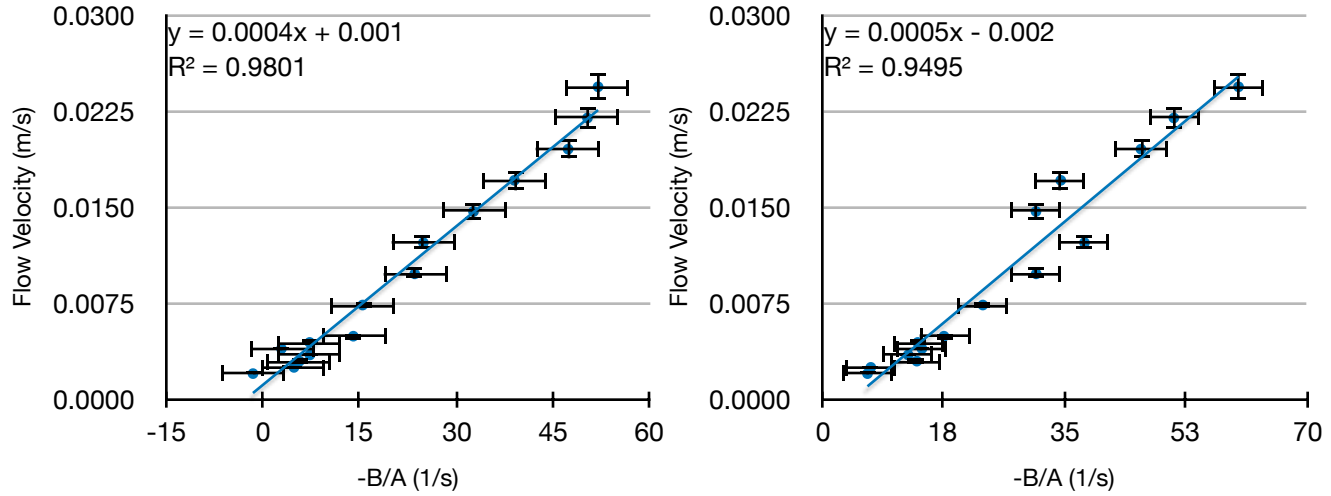

Figure 10: Example data for τ = 60 showing the inconsistencies with the linear fit model. From top to bottom the left column displays the unaltered CPMG echo train with the first 5 echoes indicated for 0.0244 and 0.0039 m/s respectively. The right column displays the corresponding data after being divided by the zero flow data set and fitted with a linear fit. In this case the model works well for the 0.0244 m/s flow but does not for the 0.0039 m/s flow.

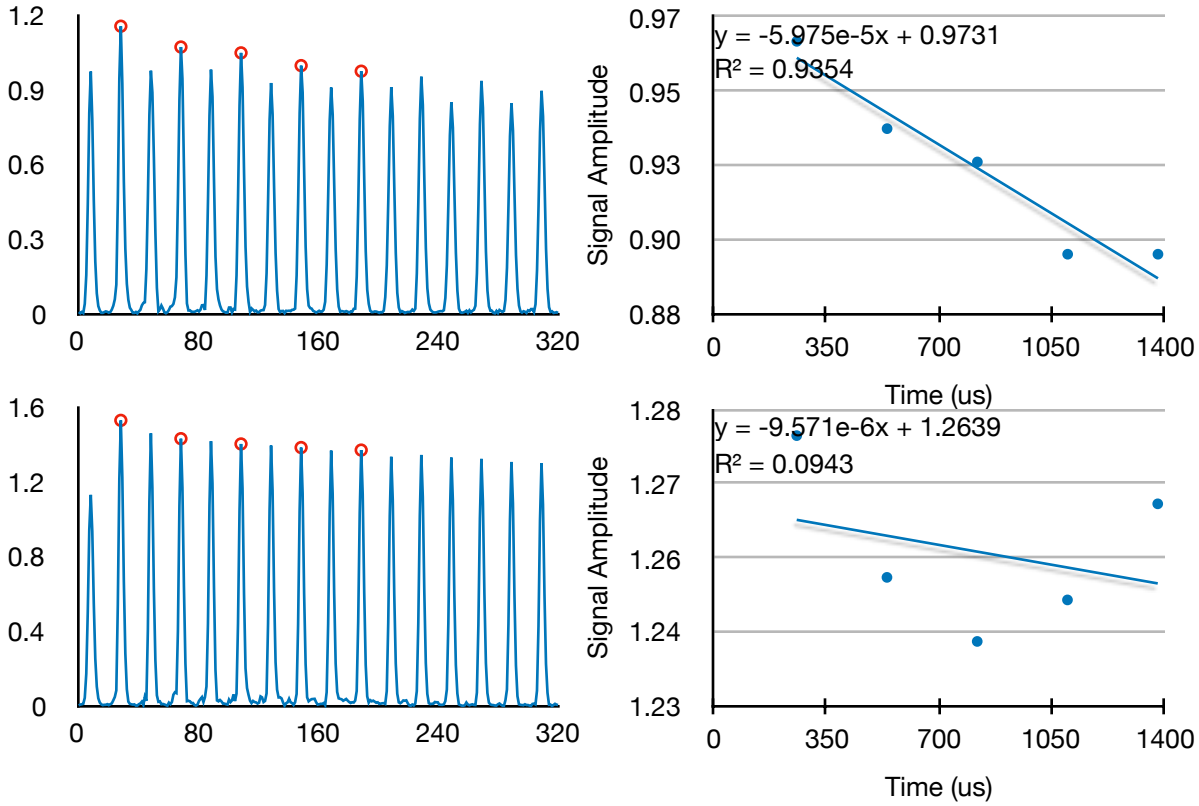

values as low as 0.0001), yet a clear linear trend was consistently observed in the -B/A vs velocity plot when the first 5 even echoes were considered. The linearity of the plot was not as consistent when 3 or 7 even echoes were considered (R^2 = 0.58 and 0.87 respectively for τ = 60 and 0.93 and 0.34 for τ = 40), yet the trend never completely disappeared. Furthermore, for all data acquisitions, the value of -B/A proved to be highly variable from one repeat to the other (see error bars in figure 9). Due to time constraints a more complex model to better describe the data was not a feasible option at the time of writing. Rather, the limits of the linear model were tested by averaging several data sets together (figure 9).

Figure 10 above shows the problem with the linear model. Despite this, as can be seen from figure 9, the model still yields a linear relationship between flow velocity and the ratio of the slope to the y-intercept.

It was observed that the overall shape of echo trains (i.e. the pattern formed by the echoes) appeared very consistent between repeats, and even small changes in velocities seemingly had a

Table 1: Results for echo train comparison method.

Flow rate	τ = 40 Predicted flow velocity (CCM)	τ = 60 Predicted flow velocity (CCM)
4CCM	7	4
5CCM	4	6
6CCM	7	9
7CCM	7	6
8CCM	9	9
9CCM	9	8
10CCM	9	9
15CCM	9	15
20CCM	20	20
25CCM	25	25
30CCM	30	30
35CCM	40	35
40CCM	40	40
45CCM	45	45
50CCM	50	50

discernible effect on the shape of the echo patterns. In order to quantitatively verify this, three repetitions with the same instrument settings were acquired for the range of flow velocities. Two of the repeats were averaged together and used as a training set for which to compare the third repeat to by normalizing the data and taking the square root of the sum of the squared differences between the echo amplitudes of the training set and the third repetition. This was done using all the flow velocities in the training set. As a result, if the echo patterns were consistent as they appeared, the smallest difference with the training set would indicate the flow velocity. The results were not as accurate as had been hoped. The results for $\boldsymbol{\tau}$ = 40 and 60 are summarized in table 1.

Future Work

The results of this work have shown that a more complex model is required to adequately describe the data. Measuring flow velocity by looking at the change in phase of the signal is also something that could be considered in the future. The end goal of this project is to design and build a practical, compact and economical NMR flow meter using common disk magnets and the techniques and knowledge gained from measuring flow using the Garfield magnet.

References

[1] "Laplacian | Garfield Magnets." *Laplacian.co.uk*. N.p., 2017. Web. 11 July 2017.

[2] Wheeler, Dustin D., and Mark S. Conradi. "Practical Exercises For Learning To Construct NMR/MRI Probe Circuits." *Concepts in Magnetic Resonance Part A* 40A.1 (2012): 1-13.

[3] "Spin-Echo And CPMG Pulse Sequence For NMR | Fundamentals Of Fluid Flow In Porous Media." *Special Core Analysis & EOR Laboratory | PERM Inc.*. N.p., 2017. Web. 11 July 2017.

[4] Osán, T.M. et al. "Fast Measurements Of Average Flow Velocity By Low-Field ^{1}H NMR." *Journal of Magnetic Resonance* 209.2 (2011): 116-122.

[5] Waluch V, Bradley WG Jr. NMR even echo rephasing in slow laminar flow. J Comput Assist Tomogr 1984; 8:594-8.

[6] "Even-Echo Rephasing." *Questions and Answers in MRI*. N.p., 2017. Web. 18 July 2017.

[7] Glover PM, Aptaker PS, Bowler JR, Ciampi E, McDonald PJ. “A Novel High-Gradient Permanent Magnet for the Profiling of Planar Films and Coatings.” Journal of Magnetic Resonance. 1999 Jul;139(1): 90-7.

Appendix I – Program List

- CPMG.PAS — Pascal source code for the implementation of the CPMG pulse sequence

CPMG.PAS parameter name	ID	Value(s)	Units
90 degree pulse	P90	1.2	us
180 degree pulse	P180	2.4	us
Probe dead time	DEAD1	27.0	us
Spectrometer frequency	SF	~33.256	MHz
Offset from signal frequency	01	281.56	Hz
Dwell time	DW	1.0	us
Receiver dead time	DEAD2	6.0	us
Sweep width	SW	1000000.0	Hz
Points per echo	SI	20	points
Number of echoes	NECH	16	
Number of scans	NS	128, 512, 2048	
Receiver Gain	RG	50.00	%
Recycle delay	RD	1000000, 5000000	us
90-180 degree pulse gap	TAU	40, 60, 150	us
90 degree pulse phase list	PH1	0213	
Receiver phase list	PH2	0213	
180 degree pulse phase list	PH3	1122	
Dummy scans	DS	0	
RF Amplitude	RFA0	56.0	Tomco amp, 12dB attenuation

Example data file name:
35CCM_Jun-21-2017_TAU=150_P90=1.2_P180=2.4_NS=512_RFA0=56_RD=1000000_CPMG.00001.RiDat

- cpmg_plotter9.m — Matlab script used for calculating -B/A ratio from data.
- cpmg_plotter13.m — Matlab script used in the echo train shape comparison analysis
- bnreadridat.m — Matlab script to read .RiDat data files generated by RI NMR into Matlab

Appendix II - τ = 150 Additional Plots

Figure 11: Plot of velocity vs. B for τ = 150 µs.

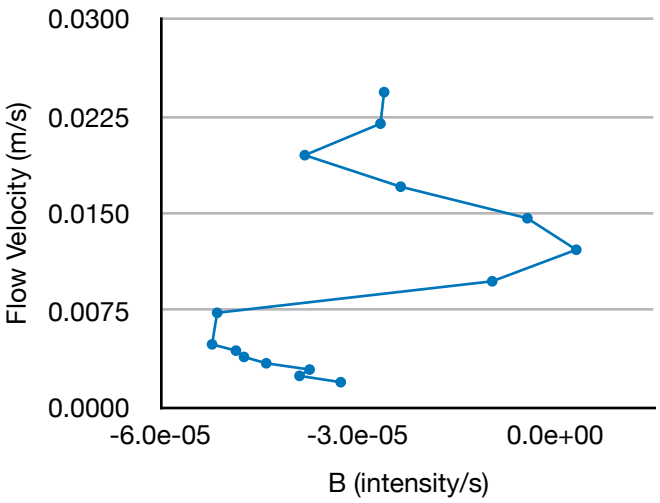

Figure 12: Plot of velocity vs. B for τ = 150 µs.

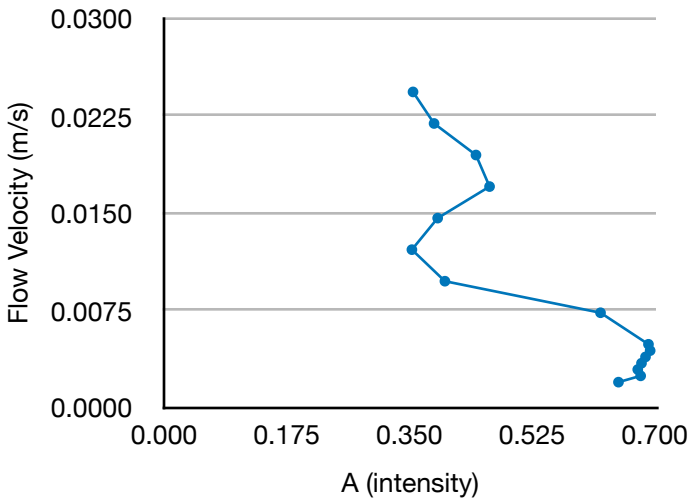

Figure 11 and 12 above respectively show the dependence of the slope of the linear fit to the first 5 echoes (B) and the y-intercept of the fit (A), on the flow velocity. Interestingly, the general trend observed in Figure 8 can be seen in both plots though it is more prominent in the plot of velocity vs B (figure 11).